Developmental Cell
Article

MATH/BTB CRL3 Receptors Target the Homeodomain-Leucine Zipper ATHB6 to Modulate Abscisic Acid Signaling

E. Lechner,[1] N. Leonhardt,[2] H. Eisler,[1,4] Y. Parmentier,[1] M. Alioua,[1] H. Jacquet,[2] J. Leung,[3] and P. Genschik[1,*]
[1]Institut de Biologie Moléculaire des Plantes, Centre National de la Recherche Scientifique, Unité Propre de Recherche 2357, Conventionné avec l'Université de Strasbourg, 67084 Strasbourg, France
[2]CEA Cadarache, DSV/DEVM/Laboratoire des Echanges Membranaires et Signalisation, UMR 6191 CNRS-CEA-Aix-Marseille-II, 13108 Saint-Paul-les-Durance Cedex, France
[3]Institut des Sciences du Végétal, Centre National de la Recherche Scientifique, Unité Propre de Recherche 2355, 1 Avenue de la Terrasse, 91198 Gif-sur-Yvette Cedex, France
[4]Present address: Vivocell Biosolutions GmbH, Stattegger Strasse 60, A-8045 Graz-Andritz, Austria
*Correspondence: pascal.genschik@ibmp-cnrs.unistra.fr
DOI 10.1016/j.devcel.2011.10.018

SUMMARY

Being sessile organisms, plants need rapid and finely tuned signaling pathways to adapt their growth and survival over their immediate and often adverse environment. Abscisic acid (ABA) is a plant hormone crucial for both biotic and abiotic stress responses. In this study, we highlight a function of six *Arabidopsis* MATH-BTB proteins in ABA signaling. MATH-BTB proteins act as substrate-binding adaptors for the Cullin3-based ubiquitin E3 ligase. Our genetic and biochemical experiments demonstrate that the MATH-BTB proteins directly interact with and target for proteasomal degradation the class I homeobox-leucine zipper (HD-ZIP) transcription factor ATHB6, which was previously identified as a negative regulator of ABA responses. Reducing CUL3^{BPM} function leads to higher ATHB6 protein accumulation, reducing plant growth and fertility, and affects stomatal behavior and responses to ABA. We further demonstrate that ABA negatively regulates ATHB6 protein turnover, a situation reminiscent to ABI5, another transcription factor involved in ABA signaling.

INTRODUCTION

Regulation of protein stability by the ubiquitin/proteasome system participates in a broad range of physiologically and developmentally controlled processes in all eukaryotes (Ciechanover et al., 2000; Smalle and Vierstra, 2004). In this pathway, a critical step involves ubiquitin ligases (E3s), which facilitate the transfer of ubiquitin moieties to substrate proteins, as a preparative step for their degradation by the 26S proteasome. Several hundred different E3s have been identified in metazoan and plant genomes, based on specific, commonly shared structural motifs. Among them, Cullin-RING E3 ubiquitin Ligases (CRLs) are the most prevalent class of E3s (Petroski and Deshaies, 2005; Hua and Vierstra, 2011). CRLs are multimeric E3s in which one distinct CULLIN protein serves as a molecular scaffold to bring together a catalytic module composed of a RING finger domain protein and an ubiquitin conjugating enzyme (E2) and a specific substrate-recognition module, which physically interacts with the target substrate(s).

CUL3 is a highly conserved CULLIN family member identified in the genome of all eukaryotes. In *Caenorhabditis elegans*, *CUL3* loss-of-function leads to a defect of cytokinesis in single-cell embryos (Kurz et al., 2002) while the deletion of this gene in mouse produces an arrest during early embryogenesis (Singer et al., 1999). In the model plant *Arabidopsis thaliana*, the disruption of the two related *CUL3* genes, called *CUL3A* and *CUL3B* also caused embryo lethality (Figueroa et al., 2005; Gingerich et al., 2005; Thomann et al., 2005).

At the structural level, CUL3 interacts with "Bric a brac, Tramtrack and Broad Complex/Pox virus and Zinc finger" (BTB/POZ, called hereafter BTB) domain proteins that function as substrate-specific adaptors (Pintard et al., 2004; Vierstra, 2009). BTB domain proteins bind CUL3, via the BTB domain and usually direct substrate specificity through an independent protein-protein interaction domain. One such domain is MATH (Meprin and TRAF homology), which serves as a recognition site for substrates of the CRL3^{MATH} subfamily of E3s (Zhuang et al., 2009). Although MATH-BTB proteins are evolutionarily conserved, their substrates are rather functionally diverse. For example, the *Drosophila* MATH-BTB protein, SPOP, recruits substrates such as the Jun Kinase phosphatase Puckered and the transcription factor Ci/Gli (Liu et al., 2009; Zhang et al., 2006), or in mammals, the chromatin component MacroH2A (Hernández-Muñoz et al., 2005). Another well-characterized MATH-BTB protein is MEL-26 from nematode (Furukawa et al., 2003; Pintard et al., 2003; Xu et al., 2003). MEL-26 recruits MEI-1, a protein with microtubule-severing activity that is required for meiotic spindle formation, but must be quickly degraded prior mitosis.

A striking feature of the MATH-BTB class of adaptors is that they largely expanded and diversified during evolution in some worm and plant species (Stogios et al., 2005; Thomas, 2006;

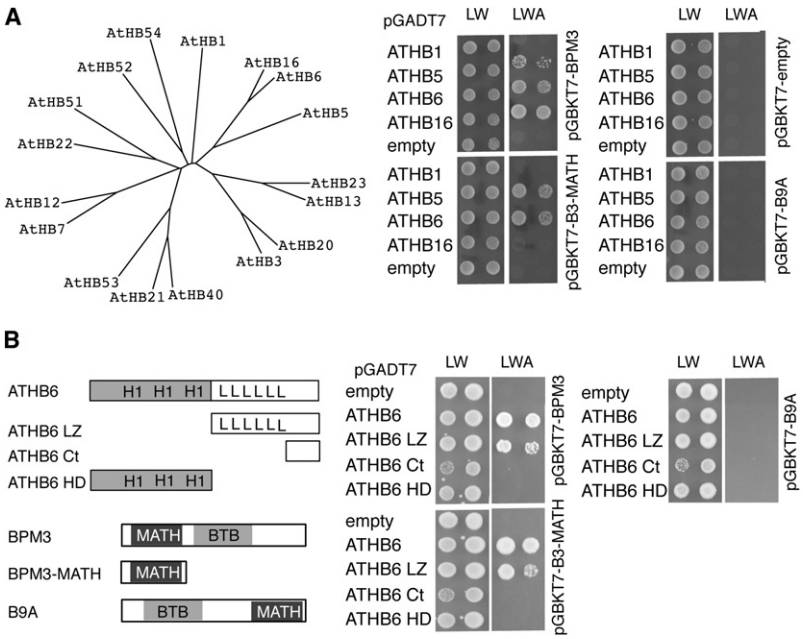

Figure 1. BPM3 Interacts with ATHB6 and Additional Members of Class I HD ZIP Transcription Factor Family

(A) Phylogenetic tree (left panel) of *Arabidopsis* HD-ZIP class I domain proteins. Clustal X 1.83 (Thompson et al., 1997) was used to align *Arabidopsis* HD-ZIP class I proteins and to compute the unrooted tree by the neighbor joining method. Complete protein sequences were used to construct the tree, gaps were taken into account for the computation and no correction was applied for multiple substitutions. The tree was then drawn using the Phylodendron 0.8d web service (http://iubio.bio.indiana.edu/soft/molbio/java/apps/trees/).

Yeast two hybrid interactions (right panel): Full-length BPM3, the MATH domain of BPM3 or B9A were tested pairwise with several *Arabidopsis* HD-ZIP class I proteins, including ATHB1, ATHB5, ATHB6, and ATHB16. Growth on selective plates lacking leucine, tryptophan and adenine (-L-W-A) and on control plates lacking only leucine and tryptophan (-L-W) is shown. Picture of the plates were taken after 4 days at 28°C.

(B) A schematic representation (left panel) of different ATHB6 deletion constructs (homedomain [HD], leucine zipper [LZ], or C terminus [Ct]) that were tested pair wise by yeast two hybrid (right panel) with the full-length BPM3, the MATH domain of BPM3 or BTB9A. Growth on selective plates lacking leucine, tryptophan, and adenine (-L-W-A) and on control plates lacking only leucine and tryptophan (-L-W) is shown. Picture of the plates were taken after 4 days at 28°C.

See also Figure S1.

Gingerich et al., 2007). For instance, while the *Arabidopsis* genome encodes six MATH-BTB proteins (hereafter called BPM1-6; Weber et al., 2005), this family has significantly expanded to 74 members in rice during evolution (Gingerich et al., 2007). This possible positive selection during evolution of MATH-BTBs has been compared to pathogen proteins that are themselves under strong positive selection (Thomas, 2006; Gingerich et al., 2007).

At present, substrates of plant MATH-BTB proteins are unknown. Here, we show that all six *Arabidopsis* BPMs physically interact with a specific subclade of class I homeodomain leucine zipper (HD-ZIP) transcription factors, including ATHB6 revealed to be involved in phytohormone abscisic acid (ABA) responses (Himmelbach et al., 2002). ABA regulates many aspects of plant growth and development including seed dormancy and germination, reproduction and is also a key component of plant responses to biotic and abiotic stress, in particular cold, salinity and drought (Yamaguchi-Shinozaki and Shinozaki, 2006; Ton et al., 2009; Cutler et al., 2010; Hubbard et al., 2010; Raghavendra et al., 2010).

ATHB6 appears to negatively regulate a subset of ABA responses, such as sensitivity toward ABA during seed germination and stomatal closure. Here, we report that a strong reduction of BPM transcript accumulation, using an artificial microRNA strategy, leads to increased ATHB6 protein content. Conversely, overexpression of BPM3 decreases the abundance of the ATHB6 protein and also suppresses phenotypic alterations, such as leaf serration and reduced growth, caused by ATHB6 ectopic expression. Moreover, we show that knockdown of BPMs as well as the overexpression of ATHB6 alters stomatal behavior under stress and non-stress conditions. Overall, our data highlight a function of $CRL3^{MATH-BTB}$ ubiquitin E3 ligases in ABA responses.

RESULTS

BPMs Interact with Members of Class I HD-ZIP Family of Transcription Factors

To identify proteins that are potentially regulated by BPMs, we conducted a yeast two-hybrid screen. The full-length coding sequence of *BPM3* fused to the binding domain of *GAL4* was used to screen a cDNA library prepared from *Arabidopsis* inflorescences. From over a two million clones screened, 125 were identified as potential interactors. Among them, 80 were subsequently confirmed by retransformation into yeast. A large class of them (approximately one-third) corresponded to BPM3 itself indicating that this protein homodimerizes, which has been previously reported (Weber et al., 2005). Interestingly, among the BPM3 interactors we also identified 13 and 2 clones corresponding to the homeobox-leucine zipper (HD-ZIP) transcription factors ATHB6 (At2g22430) and ATHB5 (At5g65310), respectively. In *Arabidopsis* HD-ZIP proteins have been grouped into four different classes (Ariel et al., 2007), ATHB6 and ATHB5 belonging to class I. Moreover, we found that BPM3 also interacts with ATHB16, but not with ATHB1, suggesting that this interaction is specific to only a subclade of class I HD-ZIP proteins (Figure 1A).

We then tested whether ATHB6 only interacts with BPM3 or whether it also interacts with additional members of the BPM family (Weber et al., 2005). Thus, all six full-length BPM coding sequences were tested for interaction with ATHB6 in yeast two hybrid assays. ATHB6 interacts with all members of the *Arabidopsis* BPM protein family (see Figure S1A available online),

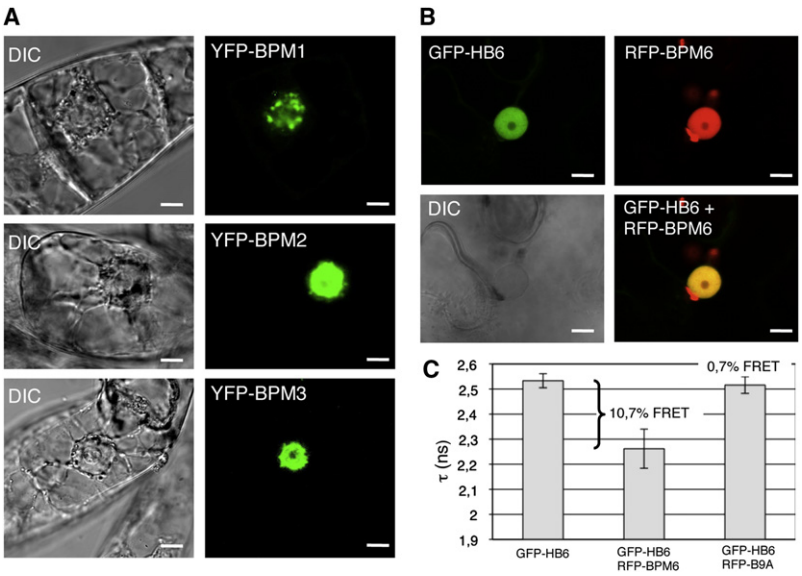

Figure 2. BPM Proteins Interact with ATHB6 in the Nuclear Compartment of the Cells

(A) Confocal images showing the subcellular distribution of YFP-tagged BPM1, BPM2, BPM3 fusion proteins in transiently transformed BY2 cells. Scale bars represent 10 μm.

(B) Confocal images showing the subcellular localization of GFP-ATHB6 and RFP-BPM6 proteins in transiently transformed tobacco cells. *Nicotiana benthamiana* plants were infiltrated with *Agrobacteria* harboring the different plasmids. The two fusion proteins colocalize in the nucleus. Scale bars represent 10 μm.

(C) FRET analysis showing that GFP-ATHB6 interacts with RFP-BPM6 in the nuclei of *N. benthamiana* cells agro-infiltrated leaves. Bars represent mean fluorescence lifetime (t, in ps ± SE) of GFP-ATHB6 alone or together with RFP-BPM6 or RFP-B9A. Mean FRET value (percentage) is indicated above the bars.

but not with B9A (At2g46260), a more distant member of this BTB protein family (Dieterle et al., 2005). To further confirm these interactions, we performed in vitro pull down assays. For this purpose, we generated GST protein-fusions with all six BPMs that were expressed in *Escherichia coli* and subsequently purified. The ATHB6 protein labeled with [^{35}S] methionine was produced in wheat germ extract. These assays showed that ATHB6 was pulled down with all BPMs, but not with GST alone nor with the unrelated B9A BTB protein (Figure S1B). It is noteworthy that the in vitro binding efficiencies were not equal, with BPM6 showing the strongest binding to ATHB6, whereas in yeast cells the strongest interactions were observed with BPM1 and BPM3. From these experiments, we conclude that ATHB6 interacts with all six members of the BPM family.

When we transiently expressed in tobacco BY2 cells BPM proteins fused at their N terminus to YFP, we observed a clear nuclear enrichment of all proteins as illustrated for BPM1-3 (Figure 2A). We also found the occasional appearance of these proteins in nuclear speckles. To confirm the interactions between BPMs and ATHB6 in planta, we used fluorescence resonance energy transfer (FRET) assays in *Nicotiana benthamiana* leaves. These assays revealed a direct interaction in the nuclei between BPM6 and ATHB6, which was not the case for B9A and ATHB6 (Figure 2B). Thus, CRL3$^{MATH-BTB}$ E3 ligases may directly ubiquitylate ATHB6 in the nucleus prior its degradation by the proteasome.

Next, we narrowed down the domain in ATHB6 that interacts with BPMs. We created a series of deletion constructs in ATHB6 that were tested for yeast two-hybrid interactions with the full-length BPM3 or the MATH domains alone (Figure 1B). These assays revealed that the MATH domain of BPM3 interacts with the leucine zipper domain of ATHB6, but not with its homeodomain (HD). Thus, the interaction between BPMs and ATHB6 may interfere with the dimerization of ATHB6 with other HD-Zip proteins, but not or only indirectly with its binding to DNA that is assumed by the HD.

BPM Genes Exhibit a Similar Pattern of Expression in a Broad Variety of Plant Tissues

We examined *BPM1-6* relative expression levels and tissue specificities by quantitative real-time RT-PCR (q-RT-PCR) and promoter-GUS fusion studies. All six *BPMs* are expressed at various levels in plant organs (Figure S2A). Moreover, these genes exhibit similar organ-specific expression patterns. In particular, *BPMs* are expressed significantly higher in floral buds and open flowers. This apparent coregulation of *BPM* genes was also apparent at the tissue specific level (Figure S2B). We cloned upstream of the *GUS* (β-glucuronidase) gene a 1–1.8 kb promoter sequence of each *BPM*, and at least ten independent transgenic lines for each construct were selected. GUS staining was detected in cotyledons, leaves, the vasculature of stems and roots, flower organs including sepals, petals, filaments, and stigma of T3 transgenic lines. A strong GUS expression was also detected in mature pollen with BPM1, 2, and 3 and to a lesser extent with BPM6. Overall, *BPM* genes are expressed in all organs with similar tissue-specific expression patterns. Our analysis is also consistent with available microarray data (Hruz et al., 2008) and other recently reported studies (Weber and Hellmann, 2009). Since all BPMs interact with ATHB6 and are coexpressed in most plant tissues, we anticipated functional redundancy among this gene family.

BPM Silencing by Artificial microRNAs and ATHB6 Overexpression Affect Plant Development in a Similar Way

To get insights into the function of *Arabidopsis* BPMs, we first examined all corresponding T-DNA insertion mutant lines from public collections. Homozygous mutants for each insertion line were produced and analyzed for BPM transcripts accumulation. Thus, four T-DNA mutant lines (BPM3: SALK072848; BPM5: SALK002733 and SALK038417; BPM6: SALK118960) led to a significant reduction in *BPM3*, *BPM5*, and *BPM6* expression. However, none of them exhibited an abnormal phenotype when grown under our conditions. To overcome the lack of multiple knockout mutants, we used a strategy based on artificial microRNAs (Parizotto et al., 2004). BPM nucleotide sequences

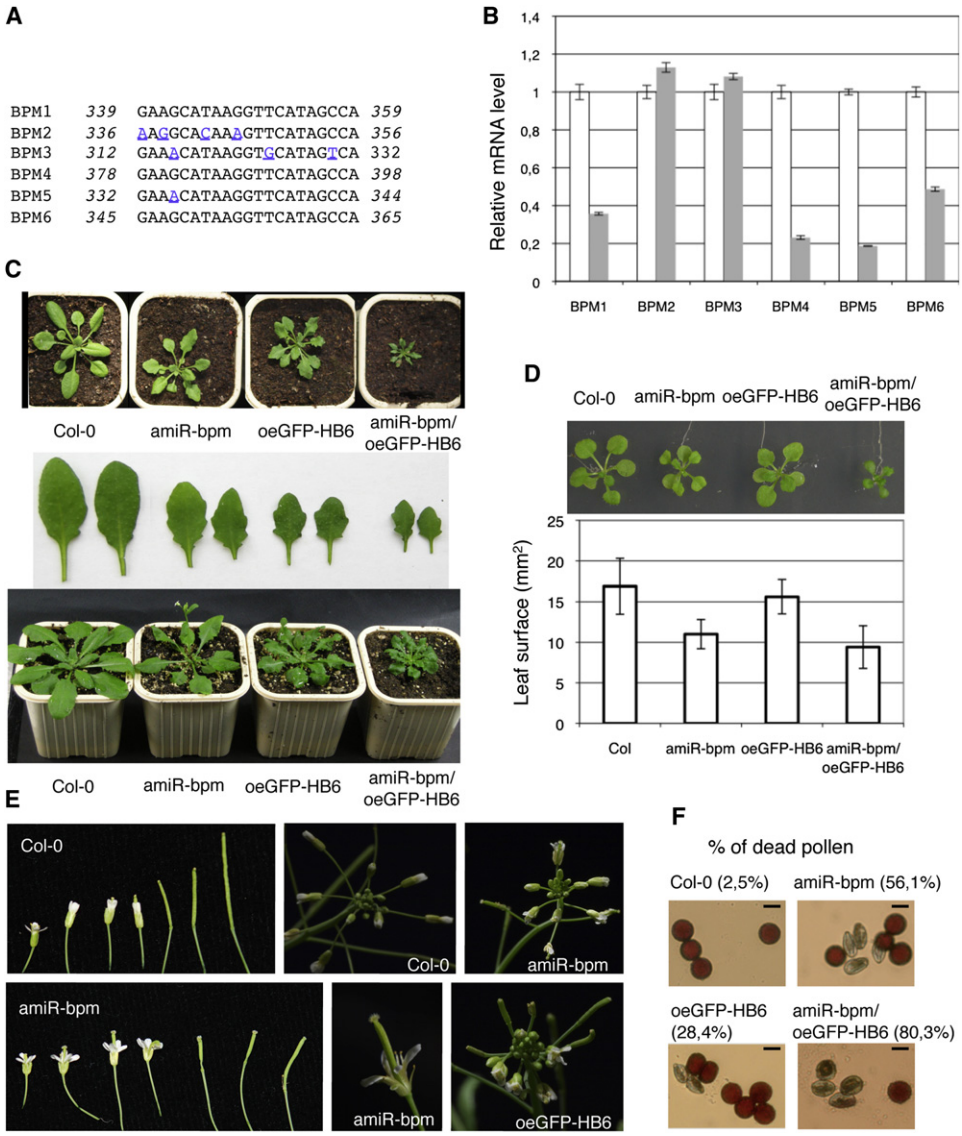

Figure 3. Downregulation of *BPM* Expression and *ATHB6* Overexpression Affect Plant Growth and Development

(A) Nucleotide sequence alignment between the sequence of the selected artificial microRNA and all six different *BPM* genes. *BPM1*, *BPM4*, and *BPM6* show a perfect sequence match with the sequence of the artificial MicroRNA. Nucleotides with mismatch are underlined.

(B) Analysis of the relative expression levels of *BPM1*, *BPM2*, *BPM3*, *BPM4*, *BPM5*, and *BPM6* gene transcripts determined by quantitative RT-PCR in 14-day-old wild-type (Col-0, white bars) and amiR-bpm line (gray bars). Data shown are means ± SD of three replicates. Similar results were obtained in three independent experiments.

(C) Phenotype of 5-week-old (upper panel) and 8-week-old (lower panel) wild-type, amiR-bpm, oeGFP-HB6, and amiR-bpm/oeGFP-HB6 plants. Pictures of two leaves corresponding to F9 and F10 from 5-week-old light grown wild-type, amiR-bpm, oeGFP-HB6, and amiR-bpm/oeGFP-HB6 plants (middle panel).

(D) Pictures of 2-week-old in vitro light grown wild-type, amiR-bpm, oeGFP-HB6 and amiR-bpm/oeGFP-HB6 seedlings (upper panel). Leaf surface measurements made on leaves F2 and F3 of 10-day-old light grown seedlings of wild-type, amiR-bpm, oeGFP-HB6, and amiR-bpm/oeGFP-HB6 plant (lower panel). Data shown are means ± SD (n = 30). It is noteworthy that the reduction in leaf size of oeGFP-HB6 plants became only apparent after 2 weeks of plant development.

(E) Pictures of flowers, siliques, and inflorescences of wild-type, oeGFP-HB6, and amiR-bpm plants.

(F) Analysis of pollen viability by transmitted light microscopy after Alexander staining on mature flowers. Two hundred to 300 pollen grains coming from four different plants of each genotype have been analyzed. Scale bars represent 10 μm.

See also Figure S2.

were aligned and we determined a 21 nucleotide-long sequence (Figure 3A), which shows a perfect match for BPM1, 4 and 6. This 21-mer was confirmed to be a good candidate sequence using Web MicroRNA designer (http://rna.tbi.univie.ac.at/cgi-bin/RNAfold.cgi). We used the miRNA171 precursor as a backbone for amiR-bpm expression under the control of the CaMV 35S promoter. Transformed plants were selected and 7 out of 20 lines showed growth and developmental alterations (Figure 3). These transgenic lines were further characterized for BPM expression and all amiR-bpm lines, as illustrated for one of

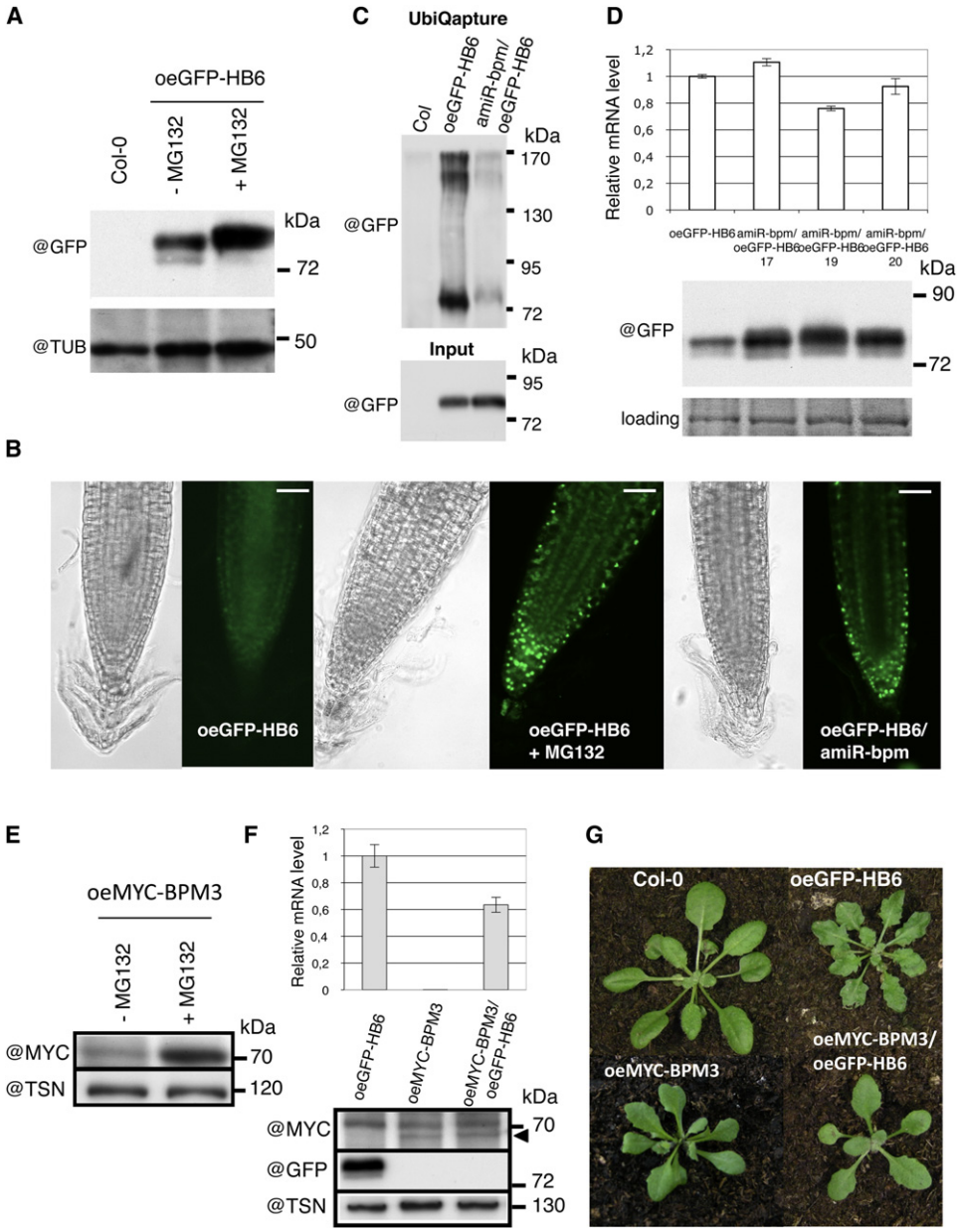

Figure 4. BPMs Trigger Proteasomal-Dependent Degradation of ATHB6 In Planta

(A) The proteasome inhibitor MG132 stabilizes ATHB6. Fourteen-day-old wild-type or oeGFP-HB6 seedlings were treated or not during 3 hr with 100 μM MG132. Total protein extracts were subjected to immunoblot assays using anti-GFP and antitubulin (as loading control) antibodies.

(B) The GFP-ATHB6 protein is stabilized in root cell nuclei treated 3 hr with 50 μM MG132, but also in nontreated amiR-bpm root cell nuclei. Fluorescence images were obtained by confocal microscopy performed on roots of 5-day-old seedlings. Scale bars represent 50 μm.

(C) UbiQapture-Q matrix was used to pull-down all ubiquitylated proteins present in a total protein sample extracted from Col-0 or from oeGFP-HB6 or from amiR-bpm/oeGFP-HB6 trangenic plants. Twice as much total protein extract of oeGFP-HB6 compared with total amiR-bpm/oeGFP-HB6 protein extract has been loaded on the UbiQapture matrix in order to perform this assays with a similar amount of ATHB6 protein in input samples. Western blot analysis using anti-GFP antibody was used to monitor the GFP-ATHB6 protein and its ubiquitylated form, which is clearly enriched in the ubiquitin-bounded fraction. When ATHB6 is expressed in the amiR-bpm background, the level of ubiquitylated ATHB6 present in the ubiquitin-bound fraction was significantly reduced.

(D) The GFP-ATHB6 protein accumulates at higher levels in different amiR-bpm lines. The relative expression levels of GFP-ATHB6 transcripts in the amiR-bpm and three independent amiR-bpm/oeGFP-HB6 lines (indicated 17, 19, and 20) were determined by quantitative RT-PCR (upper panel). Data shown are means ± SD of three replicates. Total protein extracts from the same lines were subjected to immunoblot assays using anti-GFP antibody (lower panel). Coomassie blue staining is shown as loading control.

(E) The proteasome inhibitor MG132 stabilizes BPM3. 14-day-old seedlings expressing MYC-BPM3 were treated or not during 3 hr with 100 μM MG132. Total protein extracts were subjected to immunoblot assays using anti-MYC and anti-TSN (as loading control) antibodies.

(F) Overexpression of MYC-BPM3 promotes ATHB6 protein degradation. Relative expression levels of GFP-ATHB6 transcripts in the different genetic backgrounds (as indicated) were determined by quantitative RT-PCR (upper panel). Data shown are means ± SD of three replicates. Total protein extracts from the

them (Figure 3B), exhibited a strong reduction in transcript accumulation of BPM1, 4, 5, and 6, respectively.

The phenotypic analysis of amiR-bpm plants revealed that BPMs are required for normal plant development (Figures 3C–3E). Thus, both leaf shape and leaf size were affected in these lines. The leaf blade area was reduced about 30% as compared with wild-type and mature leaves were typically serrated (Figure 3C and 3D). Moreover, the overall stature of amiR-bpm plants was reduced and appeared bushy, indicating that both stem elongation and branching were altered. The most severe phenotype was observed at the time of plant reproduction, as amiR-bpm plants exhibited alteration in flower development (Figure 3E), such as shorter pedicels, exaggerated opening of flowers, shorter stamens, protruding gynoecium, and predominantly short siliques. The reduced fertility was most likely the consequence of reduced pollen viability (Figure 3F) and stamen elongation.

We speculated that ATHB6 and eventually other class I HD-ZIP proteins are targets of $CUL3^{BPM}$ E3 ubiquitin ligases. No antibody against ATHB6 is currently available and our attempts to produce such an antibody failed, thus we fused the GFP to the N terminus of ATHB6 and expressed the chimeric protein in *Arabidopsis* under the control of the constitutive 35S promoter. Twenty independent 35S:GFP-ATHB6 *Arabidopsis* transformants (called oeGFP-HB6) were selected and further characterized. Interestingly a high proportion of these plants (~30%) showed a phenotype reminiscent to the amiR-bpm lines. In particular, oeGFP-HB6 lines showed growth retardation, presence of serrated leaves, reduced fertility and pollen viability (Figures 3C–3F). This suggests that at least some of the developmental defects observed in the amiR-bpm lines may actually result from a higher ATHB6 protein accumulation.

Ubiquitylation and Subsequent Degradation of ATHB6 Requires the Function of $CRL3^{BPM}$

The ubiquitin proteasome system (UPS) is involved in the rapid degradation of many short-lived proteins especially transcription regulators (Vierstra, 2009). To test whether ATHB6 is a UPS target, we first treated *Arabidopsis* oeGFP-HB6 lines with the proteasome inhibitor MG132. Immunoblot analysis of untreated plants revealed that ATHB6 protein shows at least two protein bands with different electrophoretic mobility (Figure 4A). After 180 min of MG132 treatment, the level of ATHB6 protein markedly increased supporting that its degradation is proteasome dependent. Consistently, when oeGFP-HB6 transgenic plants were treated with MG132, the drug promoted a strong nuclear accumulation of the protein in root tip cells (Figure 4B). To investigate whether ATHB6 is ubiquitylated, we used a specific ubiquitin-binding affinity matrix (UbiQapture), which allows purification of ubiquitylated proteins with high affinity. Ubiquitylated ATHB6 protein forms were indeed captured by the matrix as revealed by anti-GFP antibodies (Figure 4C). In addition to the polyubiquitin forms detected, we also noticed that the ubiquitin-binding affinity matrix allowed the purification of a lower molecular form of modified ATHB6. Whether this form corresponds to ATHB6 monoubiquitylation remains to be established. Moreover after immunoprecipitation, ATHB6 polyubiquitin and eventually monoubiquitin modifications were detected using an anti-UBI antibody (Figure S3).

Next, to examine whether BPM knockdown in the amiR-bpm lines affects ATHB6 protein accumulation, we used the oeGFP-HB6 line 126 to cross to three different amiR-bpm lines. After the selection of plants containing both transgenes, we measured and compared the level of ATHB6 protein in the different genetic backgrounds. As shown in Figures 4B and 4D, the GFP-ATHB6 protein levels were higher in the amiR-bpm lines than in wild-type, while the transcript levels of the transgene were similar. Consistently with a reduced turnover of the ATHB6 protein in the amiR-bpm line, we also observed a significant decrease of its ubiquitylation (Figure 4C). Strikingly, the developmental defects due to GFP-ATHB6 overexpression were dramatically enhanced when the transgene was expressed in the amiR-bpm lines (Figures 3C–3F), indicating an ATHB6 dosage dependency of the phenotype. Thus, plants expressing both transgenes showed a more pronounced inhibition of growth, a more severe reduction in fertility and pollen viability. These data indicate that reduced BPM activity leads to increased ATHB6 protein content, and thereby causing the enhanced phenotypes.

Overexpression of BPM Proteins Promotes ATHB6 Protein Degradation

To further demonstrate the role of BPMs in ATHB6 protein turnover, we produced *Arabidopsis* transgenic plants expressing *myc*-epitope-tagged BPM3 (called oeMYC-BPM3) under the control of the CaMV 35S promoter. Most transgenic oeMYC-BPM3 lines appeared similar to wild-type plants, though we observed also some slightly smaller plants in several transgenic lines with a subtle leaf serration phenotype. Despite a 3-fold increase in the level of the transgene mRNA in comparison to the endogenous mRNA, the detection of the MYC-BPM3 protein was always difficult (Figure 4E), suggesting that the protein is very unstable. However, after MG132 treatment we observed a stronger accumulation of the MYC-BPM3 protein, indicating that this CRL3 adaptor is itself a target of the proteasome (Figure 4E). Next, we introduced the GFP-ATHB6 construct into different independent oeMYC-BPM3 lines. After the selection of plants containing both transgenes, we monitored the levels of ATHB6 and BPM3 proteins by immunodetection. Interestingly, when the epitope-tagged BPM3 protein was detected, the GFP-ATHB6 protein was undetectable despite the presence of its transcript (Figure 4F), indicating that BPM overexpression stimulates ATHB6 protein degradation. Consistently, BPM3 overexpression not only promoted ATHB6 degradation, but also suppressed the phenotypic alterations caused by ATHB6 overexpression (Figure 4G). Taken together, these results reveal that ATHB6 is regulated by BPMs at the posttranslational level by mediating its proteasome-dependent degradation.

same lines were subjected to immunoblot assays using the following antibodies: anti-MYC for BPM3 detection, anti-GFP for ATHB6 detection, and anti-TSN as loading control (lower panel). The arrow indicates the MYC-BPM3 protein band.
(G) Picture of 5-week-old light grown wild-type, oeGFP-HB6, oeMYC-BPM3, and oeMYC-BPM3/oeGFP-HB6 plants.
See also Figure S3.

BPM Function Is Necessary for ABA Responses

ATHB6 is a transcription factor that negatively regulates ABA signaling (Himmelbach et al., 2002). Therefore, we aimed to characterize the function of BPMs in plant responses to this phytohormone. We first examined the inhibition of germination by ABA in our different transgenic lines. As previously reported, ATHB6 overexpression leads to ABA insensitivity, though to a lesser extent than in *abi1-1* (Himmelbach et al., 2002; Figure 5A). In agreement with BPMs negatively regulating ATHB6, the knockdown of BPMs enhanced the ABA insensitive phenotype of the oeGFP-HB6 lines. However, the amiR-bpm construct in a wild-type genetic background had no significant effects on seed germination in presence of ABA. This result suggests that endogenous ATHB6 may have only a minor role in this process, though other explanations are equally possible (see Discussion).

Next, we investigated the water loss of excised rosettes from both GFP-HB6 overexpressor and amiR-bpm lines. Interestingly, the rate of water loss was similarly increased when either ATHB6 was ectopically expressed or BPMs were downregulated (Figure 5B). Transpiration was also monitored using infrared thermography. Already at t = 0 (corresponding to the time when plant rosettes were excised), all three genotypes were colder than wild-type (Figure 5C) indicating that they lose more water in the absence of stress. Hence, ATHB6 overexpressor and amiR-bpm leaves were, respectively, 1.9°C and 1.4°C colder than those of the wild-type. This difference in leaf temperature is similar to the mutation of the ABA-activated kinase OST1/SnRK2.6 (Mustilli et al., 2002). Five minutes after dehydration stress induction, while the temperature of Col-0 increases as a consequence of stomatal closure, this was not observed in the transgenic lines, suggesting that ATHB6 regulation by BPMs is important for stomatal functions.

To investigate whether BPMs are expressed in stomata, we took advantage of the previously established microarray expression profiles of isolated guard cells (Leonhardt et al., 2004). All BPMs were found expressed in guard cells and several of them even at a higher level than in mesophyll cells (Figure S4A). An ABA treatment had, however, only a minor effect on their transcript accumulation. A strong expression of BPMs in guard cells was further confirmed by histochemical analyses of the established BPM promoter:GUS lines (Figure S4B). It is also known that ATHB6 is strongly expressed in stomata (Söderman et al., 1999; Figure S4A).

Both stomatal density (number of stomata per mm^2) and stomatal index (ratio of stomata to epidermal cells) measured on the abaxial leaf surfaces were reduced in ATHB6 overexpressor and in the double oeGFP-HB6/amiR-bpm lines (Figures S4C and S4D). This indicates that the increased transpiration in these two genotypes was not due to larger number of stomatal complex, neither in absolute numbers nor at the expense of other epidermal cell types. As a next step, we therefore examined stomatal behavior of our different transgenic lines on epidermal peels collected at the end of the night. While stomata appeared normal in shape and size, we noticed that they were more open in all different transgenic lines in comparison to wild-type (Figure 5D). In darkness, both ATHB6 overexpressor and amiR-bpm lines exhibited larger stomatal aperture (Figure 5E). This phenotype was exacerbated when ATHB6 was expressed in the amiR-bpm genetic background. After illumination, all transgenic lines were able to open their stomata, though stomatal aperture remained larger than in wild-type. Similarly, ATHB6 overexpressor and amiR-bpm lines responded to 10 μM ABA, though to a lesser extent than wild-type. Interestingly the double oeGFP-HB6/amiR-bpm line was insensitive to ABA treatment. Overall, our findings support an important function of $CRL3^{BPMs}$ E3s and their target ATHB6 in guard cell regulation under stress and nonstress conditions.

The Expression of Several ABA-Responsive Genes Is Altered in oeGFP-HB6 and amiR-bpm Lines

Several lines of evidence indicate that ATHB6 acts as a transcriptional regulator of ABA responses (Himmelbach et al., 2002). Thus, we investigated by quantitative real-time PCR the expression of three ABA-inducible HD-ZIP genes, *ATHB6* itself, *ATHB7* and *ATHB12* (Olsson et al., 2004), as well as *RD29B*, *RAB18*, and *RD22*, three well-established salt-, drought-, and ABA-responsive genes (Lång and Palva, 1992; Yamaguchi-Shinozaki and Shinozaki, 1993; Abe et al., 2003). As expected, *ATHB6*, *ATHB7*, *ATHB12* induction of gene expression by ABA was lost in *abi1-1* (not shown). However, in all transgenic lines, the endogenous *ATHB6*, *ATHB7*, and *ATHB12* transcripts are induced by ABA, although their basal level of expression is generally higher before ABA treatment when compared with wild-type plants (Figure 6A). Conversely, in the absence of ABA the basal level of expression of *RAB18*, *RD29B*, and *RD22* was significantly lower in all three transgenic lines compared with that of the wild-type, although ABA-dependent induction of gene expression could still be observed (Figure 6A). It is noteworthy that after 3 hr of ABA treatment, the level of *RAB18* expression in amiR-bpm and amiR-bpm/oeGFP-HB6 lines is still lower than its basic expression level in nontreated Col-0 plants. Thus, in line with the drought-sensitive performance of amiR-bpm, oeGFP-HB6 and amiR-bpm/oeGFP-HB6 lines, the expression of *RAB18*, *RD29B*, and *RD22* genes was attenuated in these lines.

While ABA induces *ATHB6* mRNA accumulation, we investigated whether it also affects ATHB6 protein stability. Thus, we examined ATHB6 protein half-life using the protein synthesis inhibitor cycloheximide (CHX) in the absence or in presence of 10 μM ABA. As shown in Figure 6B, ABA stabilizes ATHB6.

DISCUSSION

Role of ATHB6 and BPMs in ABA Signaling

An important breakthrough was the recent identification of the PYR/RCAR ABA receptors, which together with the clade A PROTEIN PHOSPHATASE 2Cs (PP2Cs) and the class III SNF1-RELATED PROTEIN KINASE 2 s (SnRK2s) form the primary module for early ABA signaling. Directly downstream of this signaling module are different classes of proteins including transcription factors (for review, see Cutler et al., 2010). Several bZIP transcription factors are directly phosphorylated by SnRK2s, affecting both their activity and stability (Furihata et al., 2006; Sirichandra et al., 2010). Interestingly, ATHB6, a member of the class I HD-Zip family of transcription factors, physically interacts with the PP2C phosphatase ABI1, suggesting that it is also an upstream component in ABA signaling (Himmelbach et al.,

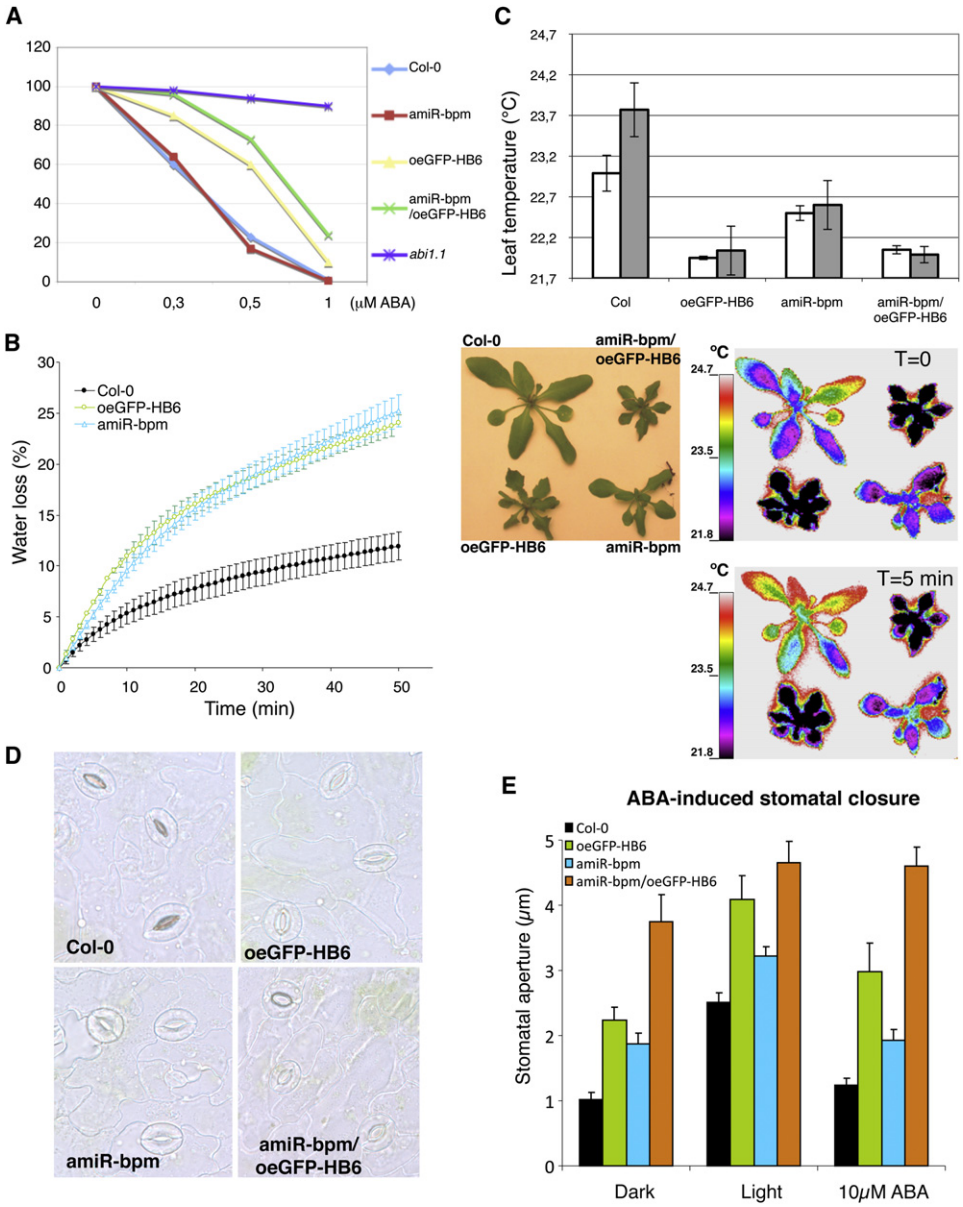

Figure 5. Downregulation of BPM Expression and ATHB6 Overexpression Affect ABA Responses

(A) Constitutive expression of ATHB6 results in ABA insensitivity in germination assays. Germination rates of Col-0, oeGFP-HB6, amiR-bpm, amiR-bpm/oeGFP-HB6, and *abi1.1* seeds exposed to 0, 0.3, 0.5, and 1 μM ABA after 5 days. Four independent experiments, with more then 150 seeds per genotype each, have been performed and gave similar results.

(B) Transpirational water loss in wild-type, oeGFP-HB6, and amiR-bpm lines at the indicated time points after detachment. Water loss is expressed as the percentage of initial fresh weight (FW). Values are means ± SD of at least three samples.

(C) False-color infrared images of Col-0, oeGFP-HB6, amiR-bpm, and amiR-bpm/oeGFP-HB6 plantlets representing leaves temperature. T = 0 denotes freshly cut rosettes and T = 5, five minutes after excision of the rosettes. Temperature of the leaf was quantified by infrared thermal imaging. Data are means ± SD (n = 5 plants for each lines, data are from ~1,000 measurements of square pixels from multiple leaves of each plant).

(D) Microscopic observation of the abaxial epidermis of Col-0, oeGFP-HB6, amiR-bpm, and amiR-bpm/oeGFP-HB6 leaves harvested in darkness at the end of the night.

(E) Col-0, oeGFP-HB6, amiR-bpm, and amiR-bpm/oeGFP-HB6 show impairment in ABA promotion of stomatal closure (n = 3 independent experiments). Error bars represent standard errors to the mean (SEM) with a confidence interval of 95%.

See also Figure S4.

2002). In addition, we found that ATHB6 also interacts with the CRL3 receptors BPM1-6 via its leucine zipper domain. Since the leucine zipper domain is also involved in the homo- and heterodimerization of the HD-ZIP proteins (Harris et al., 2011), it is possible that the binding of BPMs may interfere with their dimerization.

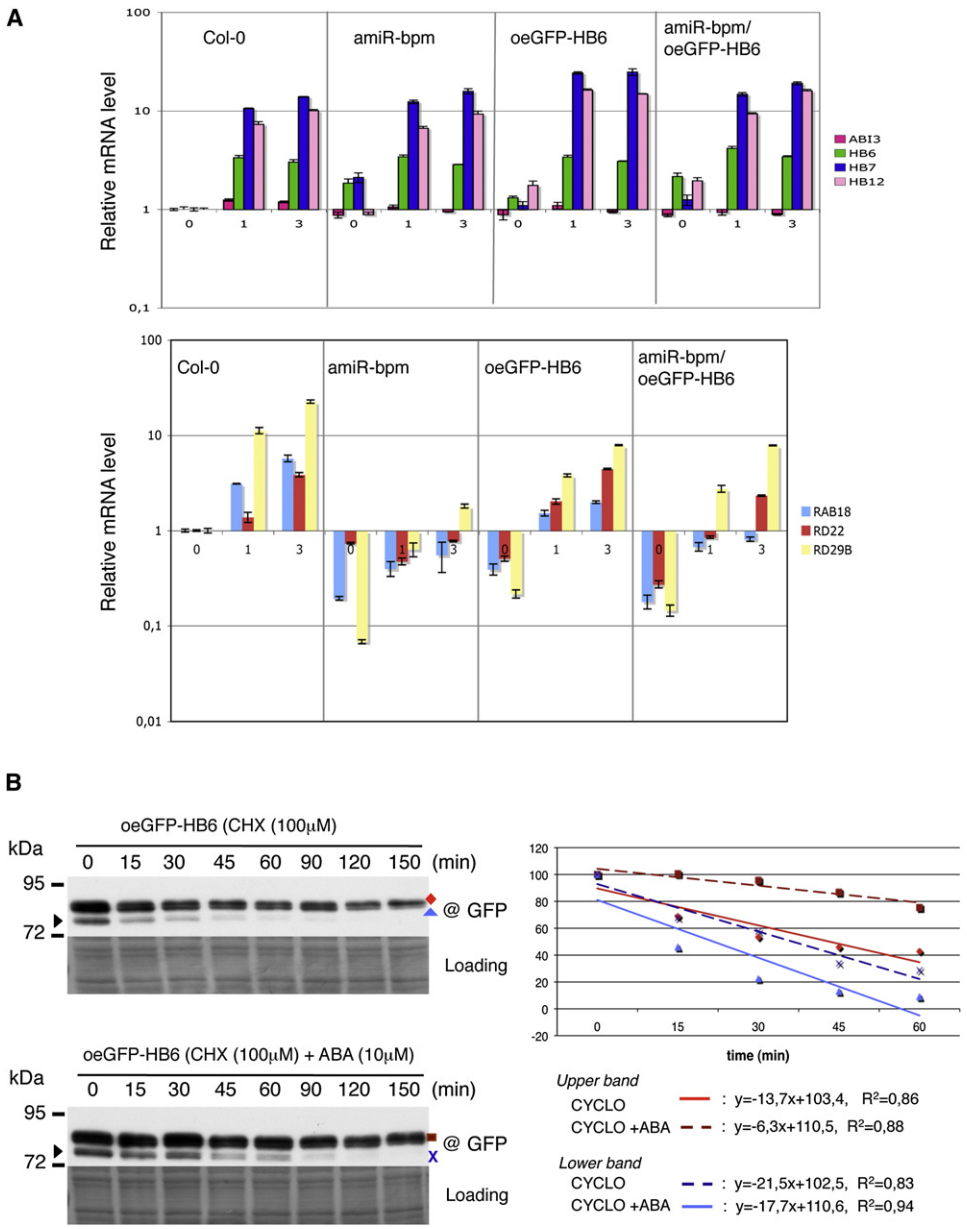

Figure 6. ATHB6 Attenuates the Expression of Several ABA-Responsive Genes and Is More Stable in Presence of ABA

(A) Relative expression levels of ABA- and drought-responsive genes (*ABI3*, *ATHB6*, *ATHB7*, *ATHB12*, *RAB18*, *RD29B*, and *RD22*) in wild-type and different transgenic lines as indicated were determined by quantitative RT-PCR. For these assays, 14-day-old seedlings were treated with 10 μM ABA for 0, 1, and 3 hr respectively. Data shown are means ± SD of three replicates.

(B) ATHB6 protein turnover decreases in the presence of ABA. Fourteen-day-old GFP-ATHB6 seedlings were transferred in liquid MS medium containing the protein synthesis inhibitor cycloheximide (100 μM) supplemented with or without 10 μM ABA. At various times (indicated in minutes), the seedlings were harvested and protein extracts were analyzed by immunoblotting using an anti-GFP monoclonal antibody (left panel). An arrow indicates the faster migrating form of ATHB6. Both bands corresponding to the higher and the lower molecular weight isoforms of ATHB6 were quantified separately using ImageJ software during cycloheximide treatment in the presence or not of ABA (right panel). All signals were normalized to the corresponding loading control bands. Characteristics of each linear regression are notified below the chart.

Here, we showed that the knockdown of BPMs and the ectopic expression of ATHB6 result in defects in stomatal closure. Furthermore, the expression of all BPMs and ATHB6 in guard cells further supports their function in stomata behavior. The regulation of ATHB6 by BPMs is, however, not restricted to stomata as plant growth, in particular, leaf growth, pedicel length, and also pollen maturation were affected in amiR-bpm and oeGFP-HB6 lines in a similar way. These developmental alterations were even more pronounced when both transgenes were combined, most likely as a consequence of a higher ATHB6 protein accumulation.

Because ATHB6 overexpression reduces ABA sensitivity both in seed germination and stomatal behavior (Himmelbach et al.,

2002 and Figure 5), ATHB6 can thus be considered as a negative regulator of the ABA signaling pathway. Consistent with this is that ATHB6 overexpression attenuated the ABA-dependent induction of *RAB18*, *RD22*, and *RD29B*. This effect was even stronger in the amiR-bpm lines, which could be explained by the stabilization of not only ATHB6, but also additional HD-ZIP transcription factor members with similar activity. In this sense, ATHB6 would be analogous to other transcriptional factors, which act as negative regulators of guard cell signaling, including the ETHYLENE RESPONSE FACTOR 7 (ERF7; Song et al., 2005) and NUCLEAR PROTEIN X1 (NPX1; Kim et al., 2009). In particular, ERF7 is believed to function as a transcriptional repressor, whose activity may be required to attenuate at least some ABA responses (Song et al., 2005). Note, however, ATHB6 is known to also act as a transcriptional activator, by directly binding to a defined *cis*-element to activate its own transcription and the transcription of other genes (Himmelbach et al., 2002). Nevertheless, ATHB6 overexpression had very little effect on its own expression in presence of ABA. This was also observed for two other HD-ZIP transcription factors tested. Therefore, as previously suggested (Himmelbach et al., 2002), ATHB6 protein per se is not sufficient to trigger transcriptional activity, but depends on other regulatory mechanisms. Together, our data indicate that ATHB6 may act during an ABA response as a transcriptional (co)activator of some genes (especially on HD-ZIP factors), while it would negatively regulate others, such as *RAB18*, *RD22*, and *RD29B*.

It is noteworthy that not all ABA functions seem to implicate ATHB6 or its regulation by the CRL3^{BPM} E3s. For instance, the inhibition of root growth by applied ABA was not affected in the oeGFP-HB6 or amiR-bpm lines (Himmelbach et al., 2002 and data not shown). Curiously for seed germination, we noticed no difference in ABA sensitivity between the control and amiR-bpm lines, while as previously reported (Himmelbach et al., 2002 and Figure 5A), ATHB6 overexpression resulted in ABA insensitivity. To explain this difference, we consider at least two possible scenarios. One possibility is that the effect on germination in oeGFP-HB6 lines is due to its ectopic expression, but that ATHB6 may have no physiological function in this process. An alternative scenario could be that during seed germination, BPM depletion in the amiR-bpm lines would result in the stabilization of ATHB5 (Johannesson et al., 2003), which also interacts with BPMs. ATHB5 was described as a positive regulator of ABA responsiveness (Johannesson et al., 2003) and since ATHB5 can heterodimerize with ATHB6, at least in vitro (Johannesson et al., 2001), ATHB5 overaccumulation could eventually counteract the effect of ATHB6 on seed germination.

CRL3^{BPM} Corresponds to a Class of E3s Involved ABA Signaling

The UPS plays a major role in all hormone-signaling pathways to fine-tune several key transcription factors (Vierstra, 2009; Santner and Estelle, 2010). ABA signaling does not escape this rule and in particular the posttranslational regulation of ABI5 attracted much attention. It was previously shown that the ABA or stress-dependent increase of ABI5 is the consequence of reduced proteolysis (Lopez-Molina et al., 2001). ABI5 protein level is also selectively stabilized in *rpn10-1*, a mutation affecting the RPN10 subunit of the 26S proteasome (Smalle et al., 2003). Subsequently an ABI5-binding protein called AFP was found to promote ABI5 degradation in nuclear bodies (Lopez-Molina et al., 2003). However, it is only recently that UPS components involved in ABI5 degradation were identified. Hence, a key player is KEEP ON GOING (KEG), an E3 containing a RING domain, which triggers ABI5 degradation to maintain its level low in the absence of stress (Stone et al., 2006). Moreover, two CRL4 substrate receptors, called DWA1 and DWA2, also physically interact with ABI5 and promote its degradation (Lee et al., 2010). Thus, ABI5 protein is fine-tuned by different classes of E3s, though their respective roles in ABA signaling remain still unclear.

Beside the fact that both ATHB6 and ABI5 interact with components of the primary module for ABA signaling (see above), these transcription factors share also a similar negative regulation by E3s at the posttranslational level. Hence, several lines of evidence indicate that CRL3^{BPM} direct the turnover ATHB6 and eventually other members of this class of transcription factors. First, all six BPM proteins are bona fide CRL3 receptors (Weber et al., 2005) and they do directly interact with ATHB6 in vitro and in vivo. Second, ATHB6 protein accumulates in plants with reduced CRL3^{BPM} activity. Third, overexpression of BPMs suppresses ATHB6 protein accumulation and at least some ABA associated phenotypes. Based on these findings we propose that CRL3^{BPM} E3s trigger ATHB6 destruction in the absence of stress, when growth conditions are favorable. This is in agreement with the constitutive expression of BPMs in several adult plant tissues and especially with their higher expression in guard cells. However, upon stress, ATHB6 protein could accumulate as a consequence of increased transcript accumulation and protein stability to trigger the expression and repression of downstream genes, which at least some are involved in ABA desensitization.

However, how ATHB6 can accumulate under such conditions is unknown. It was recently shown that KEG protein abundance is negatively regulated by ABA providing a possible explanation on how ABI5 could accumulate (Liu and Stone, 2010). However, we did not observe a negative regulation of BPMs at the transcript (all BPMs) or protein (BPM3 and BPM6) levels (not shown), suggesting that ATHB6 protein accumulation depends on another mode of regulation. One possibility is that this regulation implies ATHB6 phosphorylation. This would be consistent with the detection of at least two different ATHB6 protein forms on SDS-PAGE and the fact that ATHB6 was previously found to physically associate with the PP2C phosphatase ABI1, suggesting that it could be one of its substrate. Though ATHB6 has no predicted SnRK2 phosphorylation target sequence R-X-X-(S/T) (Furihata et al., 2006), we cannot rule out that ATHB6 is not a direct substrate of SnRK2 kinases as several of these substrates, such as the channel proteins SLAC1 and KAT1 and the NADPH oxidase AtrbohF, are phosphorylated at nonconsensus sites (Geiger et al., 2009; Sato et al., 2009; Sirichandra et al., 2009). It is, however, noteworthy that calf intestinal phosphatase had no effect on any of the ATHB6 protein forms on SDS PAGE (data not shown), a situation reminiscent of ABI5 (Liu and Stone, 2010).

Beside phosphorylation, sumoylation is another posttranslational modification (PTM) known to modulate ABA signaling.

Early studies have proposed a positive role for sumoylation in the induction of ABA-responsive genes (Lois et al., 2003). However, SUMO targets in ABA signaling were only recently identified. In particular, it was shown that ABI5 is sumoylated and that this PTM protects the inactive form of ABI5 from proteolytic degradation (Miura et al., 2009). ABI5 sumoylation depends on the SUMO E3 ligase SIZ1, which acts thus as a negative regulator of ABA signaling at least during seed germination. Interestingly, ATHB6 was also recently identified as a possible sumoylated protein in an elegant proteomic analysis (Miller et al., 2010). Future research will reveal whether sumoylation affects ATHB6 activity and/or stability in ABA signaling.

Are BPMs Only Involved in ABA Signaling?

ABI1 is a component of the core ABA signaling module. It has been previously shown that nuclear localization of ABI1 is an important prerequisite for a range of its regulatory function in ABA signaling, and surprisingly, even for quick responses such as stomatal closure (Moes et al., 2008). The association of ATHB6 with ABI1, and the ABA-dependent turnover rate of ATHB6 by $CRL3^{BPMs}$ could thus constitute a nucleus located signaling module poised to reconfigure a subset of the stress adaptive responses. Although the phenotype of plants overexpressing ATHB6 nicely mimics BPM knockdown, it is likely that ATHB6 is not the only substrate of $CRL3^{BPMs}$. In particular, it is probable that other members of class I HD-ZIP proteins are also targeted by these E3 ubiquitin ligases as two of them, ATHB5 and ATHB16, interact with BPMs, at least in yeast cells. Moreover, another yeast two-hybrid screen performed with a root specific cDNA library using BPM1 and BPM3 as baits revealed RAP2.4, a member of the ERF/AP2 transcription factor family (Weber and Hellmann, 2009). Interestingly, RAP2.4 was previously shown to mediate multiple stress responses (Lin et al., 2008). However, whether RAP2.4 represents also an in vivo target of $CRL3^{BPM}$ E3s remains to be demonstrated. Finally, since BPM proteins homo- and heterodimerize, it is possible that the complexity of this family of E3 ubiquitin ligases and the repertoire of their substrates are much broader than we had initially anticipated.

EXPERIMENTAL PROCEDURES

Standard procedures, such as plasmids constructs, yeast two-hybrid assays, GST pull-down assays, transient expression in BY2 cells, histology and microscopy analyses, FLIM, quantitative RT-PCR, protein extraction, immunoprecipitation assays, and immunoblotting are described in Supplemental Information.

Plant Material and Growth Conditions

For in vitro culture, seeds were surface sterilized using the ethanol method, plated on Germination Medium (MS salts (Duchefa, The Netherlands), 1% sucrose, 0.8% agar [pH 5.8]) in the presence or absence of a selection agent, stored 2–3 days at 4°C in the dark, and then transferred to a plant growth chamber under a 16 hr/8 hr photoperiod (22°C/20°C).

ABA germination assays were performed on GM medium without sugar supplemented with 0.3, 0.5, or 1 μM ABA). Seeds of Col-0, amiR-bpm, oeGFP-HB6, amiR-bpm/oeGFP-ATHB6, and *abi1.1* mutant were sterilized and kept for 3 days at 4°C in the dark. Germination rate was measured 5 days after transfer to a plant growth chamber under a 16 hr/8 hr photoperiod (22°C/20°C).

For soil-cultured plants, seeds were sown (20/pot) and put at 4°C in the dark during 3 days. Two weeks later, single plants were transferred to pots in the greenhouse and kept under a regimen of 16 hr/8 hr photoperiod (20°C/16°C; 70% humidity).

Stomatal Aperture Measurements

To study the promotion of stomatal closure by ABA, leaves from 4- to 5-week-old plants (grown in 8 hr of light at 22°C and 16 hr of darkness at 20°C; 70% Relative Humidity) were harvested in darkness at the end of the night. Paradermal sections of abaxial epidermis obtained were incubated in 30 mM KCl, 10 mM MES-Tris (pH 6.0), at 20°C and exposed to light for 2 hr. Subsequently, 10 μM ABA was added to the solution to assay for stomatal closing. After treatment for 3 hr, stomatal apertures were measured with an optical microscope (Nikon, Optiphot-2) fitted with a camera lucida and a digitizing table (TG 1017; Houston Instrument) linked to a personal computer. The apertures of usually 60–80 stomata were measured in each independent experiment. All experiments were repeated at least three times.

Infrared Thermography

Plants used for measurements of foliar temperature were grown in standard gardening soil purchased from local suppliers. Plants were maintained in controlled chambers at 24°C, 40% humidity, 16 hr light-dark cycle (150 $\mu E/m^2/s$). Plants were watered every second day. Infrared thermographic images of cut rosettes were acquired as described by Merlot et al. (2002).

Water Loss Measurement

For water loss measurement, rosette leaves of wild-type, oeGFP-HB6, and amiR-bpm lines were detached from their seedlings, placed in weighting dishes, and incubated on the laboratory bench. Losses in fresh weight was monitored at the indicated times. Water loss is expressed as the percentage of initial fresh weight.

UbiQapture (Enzo Life Science)

Two-week-old Columbia or oeGFP-ATHB6 or amiR-bpm/oeGFP-ATHB6 seedlings were treated for 3 hr with 20 μM of the DUB inhibitor PR-619 (Life Sensors) and with 100 μM of proteasome inhibitor MG132 (PolyPeptide Group) prior to grinding in liquid nitrogen and extraction of total proteins. UbiQapture experiments were performed following manufacturer's specifications using 300 mg of grinded plant tissue resuspended in 500 μl of lysis buffer (20 mM Sodium Phosphate buffer [pH 7.2], 1% NP-40, protease inhibitor tablets [Roche], 20 μM PR-619). The UbiQapture-Q matrix has very high ubiquitin binding characteristics (for mono-ubiquitin and polyubiquitin chains). UbiQapture-Q bound fraction was separated on SDS–PAGE gels and blotted onto Immobilon-P membrane (Millipore). GFP-ATHB6 protein was detected by using anti-GFP-HRP (Miltenyi) diluted 1:3,000 (v/v).

SUPPLEMENTAL INFORMATION

Supplemental Information includes four figures, two tables, and Supplemental Experimental Procedures and can be found with this article online at doi:10.1016/j.devcel.2011.10.018.

ACKNOWLEDGMENTS

We would like to acknowledge June Kwak for critical reading of the manuscript, Marina Bureau for technical help in microscopy, Jérôme Mutterer et Jean-Michel Davière for help with FRET imaging, Marc Bergdoll for help in phylogenetic analyses, Catherine Perrot-Rechenmann for providing the anti-TSN antibody, Tsuyoshi Nakagawa and Sumie Ishiguro for providing pGWBs gateway vectors, NASC for supplying mutant lines, and ABRC (TAIR) for cDNAs. Funding was provided by the CNRS.

Received: July 18, 2011
Revised: September 5, 2011
Accepted: October 26, 2011
Published online: December 12, 2011

REFERENCES

Abe, H., Urao, T., Ito, T., Seki, M., Shinozaki, K., and Yamaguchi-Shinozaki, K. (2003). Arabidopsis AtMYC2 (bHLH) and AtMYB2 (MYB) function as transcriptional activators in abscisic acid signaling. Plant Cell *15*, 63–78.

Ariel, F.D., Manavella, P.A., Dezar, C.A., and Chan, R.L. (2007). The true story of the HD-Zip family. Trends Plant Sci. *12*, 419–426.

Ciechanover, A., Orian, A., and Schwartz, A.L. (2000). Ubiquitin-mediated proteolysis: biological regulation via destruction. Bioessays *22*, 442–451.

Cutler, S.R., Rodriguez, P.L., Finkelstein, R.R., and Abrams, S.R. (2010). Abscisic acid: emergence of a core signaling network. Annu. Rev. Plant Biol. *61*, 651–679.

Dieterle, M., Thomann, A., Renou, J.P., Parmentier, Y., Cognat, V., Lemonnier, G., Müller, R., Shen, W.H., Kretsch, T., and Genschik, P. (2005). Molecular and functional characterization of Arabidopsis Cullin 3A. Plant J. *41*, 386–399.

Figueroa, P., Gusmaroli, G., Serino, G., Habashi, J., Ma, L., Shen, Y., Feng, S., Bostick, M., Callis, J., Hellmann, H., and Deng, X.W. (2005). Arabidopsis has two redundant Cullin3 proteins that are essential for embryo development and that interact with RBX1 and BTB proteins to form multisubunit E3 ubiquitin ligase complexes in vivo. Plant Cell *17*, 1180–1195.

Furihata, T., Maruyama, K., Fujita, Y., Umezawa, T., Yoshida, R., Shinozaki, K., and Yamaguchi-Shinozaki, K. (2006). Abscisic acid-dependent multisite phosphorylation regulates the activity of a transcription activator AREB1. Proc. Natl. Acad. Sci. USA *103*, 1988–1993.

Furukawa, M., He, Y.J., Borchers, C., and Xiong, Y. (2003). Targeting of protein ubiquitination by BTB-Cullin 3-Roc1 ubiquitin ligases. Nat. Cell Biol. *5*, 1001–1007.

Geiger, D., Scherzer, S., Mumm, P., Stange, A., Marten, I., Bauer, H., Ache, P., Matschi, S., Liese, A., Al-Rasheid, K.A., et al. (2009). Activity of guard cell anion channel SLAC1 is controlled by drought-stress signaling kinase-phosphatase pair. Proc. Natl. Acad. Sci. USA *106*, 21425–21430.

Gingerich, D.J., Gagne, J.M., Salter, D.W., Hellmann, H., Estelle, M., Ma, L., and Vierstra, R.D. (2005). Cullin 3A and B assemble with members of the broad complex/tramtrack/bric-A-brac (BTB) protein family to form essential ubiquitin-protein ligases (E3s) in Arabidopsis. J. Biol. Chem. *280*, 18810–18821.

Gingerich, D.J., Hanada, K., Shiu, S.H., and Vierstra, R.D. (2007). Large-scale, lineage-specific expansion of a bric-a-brac/tramtrack/broad complex ubiquitin-ligase gene family in rice. Plant Cell *19*, 2329–2348.

Harris, J.C., Hrmova, M., Lopato, S., and Langridge, P. (2011). Modulation of plant growth by HD-Zip class I and II transcription factors in response to environmental stimuli. New Phytol. *190*, 823–837.

Hernández-Muñoz, I., Lund, A.H., van der Stoop, P., Boutsma, E., Muijrers, I., Verhoeven, E., Nusinow, D.A., Panning, B., Marahrens, Y., and van Lohuizen, M. (2005). Stable X chromosome inactivation involves the PRC1 Polycomb complex and requires histone MACROH2A1 and the CULLIN3/SPOP ubiquitin E3 ligase. Proc. Natl. Acad. Sci. USA *102*, 7635–7640.

Himmelbach, A., Hoffmann, T., Leube, M., Höhener, B., and Grill, E. (2002). Homeodomain protein ATHB6 is a target of the protein phosphatase ABI1 and regulates hormone responses in Arabidopsis. EMBO J. *21*, 3029–3038.

Hruz, T., Laule, O., Szabo, G., Wessendorp, F., Bleuler, S., Oertle, L., Widmayer, P., Gruissem, W., and Zimmermann, P. (2008). Genevestigator v3: a reference expression database for the meta-analysis of transcriptomes. Adv. Bioinformatics. 10.1155/2008/420747.

Hua, Z., and Vierstra, R.D. (2011). The cullin-RING ubiquitin-protein ligases. Annu. Rev. Plant Biol. *62*, 299–334.

Hubbard, K.E., Nishimura, N., Hitomi, K., Getzoff, E.D., and Schroeder, J.I. (2010). Early abscisic acid signal transduction mechanisms: newly discovered components and newly emerging questions. Genes Dev. *24*, 1695–1708.

Johannesson, H., Wang, Y., and Engström, P. (2001). DNA-binding and dimerization preferences of Arabidopsis homeodomain-leucine zipper transcription factors in vitro. Plant Mol. Biol. *45*, 63–73.

Johannesson, H., Wang, Y., Hanson, J., and Engström, P. (2003). The Arabidopsis thaliana homeobox gene ATHB5 is a potential regulator of abscisic acid responsiveness in developing seedlings. Plant Mol. Biol. *51*, 719–729.

Kim, M.J., Shin, R., and Schachtman, D.P. (2009). A nuclear factor regulates abscisic acid responses in Arabidopsis. Plant Physiol. *151*, 1433–1445.

Kurz, T., Pintard, L., Willis, J.H., Hamill, D.R., Gönczy, P., Peter, M., and Bowerman, B. (2002). Cytoskeletal regulation by the Nedd8 ubiquitin-like protein modification pathway. Science *295*, 1294–1298.

Lång, V., and Palva, E.T. (1992). The expression of a rab-related gene, rab18, is induced by abscisic acid during the cold acclimation process of Arabidopsis thaliana (L.) Heynh. Plant Mol. Biol. *20*, 951–962.

Lee, J.H., Yoon, H.J., Terzaghi, W., Martinez, C., Dai, M., Li, J., Byun, M.O., and Deng, X.W. (2010). DWA1 and DWA2, two Arabidopsis DWD protein components of CUL4-based E3 ligases, act together as negative regulators in ABA signal transduction. Plant Cell *22*, 1716–1732.

Leonhardt, N., Kwak, J.M., Robert, N., Waner, D., Leonhardt, G., and Schroeder, J.I. (2004). Microarray expression analyses of Arabidopsis guard cells and isolation of a recessive abscisic acid hypersensitive protein phosphatase 2C mutant. Plant Cell *16*, 596–615.

Lin, R.C., Park, H.J., and Wang, H.Y. (2008). Role of Arabidopsis RAP2.4 in regulating light- and ethylene-mediated developmental processes and drought stress tolerance. Mol. Plant *1*, 42–57.

Liu, H., and Stone, S.L. (2010). Abscisic acid increases Arabidopsis ABI5 transcription factor levels by promoting KEG E3 ligase self-ubiquitination and proteasomal degradation. Plant Cell *22*, 2630–2641.

Liu, J., Ghanim, M., Xue, L., Brown, C.D., Iossifov, I., Angeletti, C., Hua, S., Nègre, N., Ludwig, M., Stricker, T., et al. (2009). Analysis of Drosophila segmentation network identifies a JNK pathway factor overexpressed in kidney cancer. Science *323*, 1218–1222.

Lois, L.M., Lima, C.D., and Chua, N.H. (2003). Small ubiquitin-like modifier modulates abscisic acid signaling in Arabidopsis. Plant Cell *15*, 1347–1359.

Lopez-Molina, L., Mongrand, S., and Chua, N.H. (2001). A postgermination developmental arrest checkpoint is mediated by abscisic acid and requires the ABI5 transcription factor in Arabidopsis. Proc. Natl. Acad. Sci. USA *98*, 4782–4787.

Lopez-Molina, L., Mongrand, S., Kinoshita, N., and Chua, N.H. (2003). AFP is a novel negative regulator of ABA signaling that promotes ABI5 protein degradation. Genes Dev. *17*, 410–418.

Merlot, S., Mustilli, A.C., Genty, B., North, H., Lefebvre, V., Sotta, B., Vavasseur, A., and Giraudat, J. (2002). Use of infrared thermal imaging to isolate Arabidopsis mutants defective in stomatal regulation. Plant J. *30*, 601–609.

Miller, M.J., Barrett-Wilt, G.A., Hua, Z., and Vierstra, R.D. (2010). Proteomic analyses identify a diverse array of nuclear processes affected by small ubiquitin-like modifier conjugation in Arabidopsis. Proc. Natl. Acad. Sci. USA *107*, 16512–16517.

Miura, K., Lee, J., Jin, J.B., Yoo, C.Y., Miura, T., and Hasegawa, P.M. (2009). Sumoylation of ABI5 by the Arabidopsis SUMO E3 ligase SIZ1 negatively regulates abscisic acid signaling. Proc. Natl. Acad. Sci. USA *106*, 5418–5423.

Moes, D., Himmelbach, A., Korte, A., Haberer, G., and Grill, E. (2008). Nuclear localization of the mutant protein phosphatase abi1 is required for insensitivity towards ABA responses in Arabidopsis. Plant J. *54*, 806–819.

Mustilli, A.C., Merlot, S., Vavasseur, A., Fenzi, F., and Giraudat, J. (2002). Arabidopsis OST1 protein kinase mediates the regulation of stomatal aperture by abscisic acid and acts upstream of reactive oxygen species production. Plant Cell *14*, 3089–3099.

Olsson, A.S., Engström, P., and Söderman, E. (2004). The homeobox genes ATHB12 and ATHB7 encode potential regulators of growth in response to water deficit in Arabidopsis. Plant Mol. Biol. *55*, 663–677.

Parizotto, E.A., Dunoyer, P., Rahm, N., Himber, C., and Voinnet, O. (2004). In vivo investigation of the transcription, processing, endonucleolytic activity, and functional relevance of the spatial distribution of a plant miRNA. Genes Dev. *18*, 2237–2242.

Petroski, M.D., and Deshaies, R.J. (2005). Function and regulation of cullin-RING ubiquitin ligases. Nat. Rev. Mol. Cell Biol. *6*, 9–20.

Pintard, L., Willis, J.H., Willems, A., Johnson, J.L., Srayko, M., Kurz, T., Glaser, S., Mains, P.E., Tyers, M., Bowerman, B., and Peter, M. (2003). The BTB protein MEL-26 is a substrate-specific adaptor of the CUL-3 ubiquitin-ligase. Nature *425*, 311–316.

Pintard, L., Willems, A., and Peter, M. (2004). Cullin-based ubiquitin ligases: Cul3-BTB complexes join the family. EMBO J. *23*, 1681–1687.

Raghavendra, A.S., Gonugunta, V.K., Christmann, A., and Grill, E. (2010). ABA perception and signalling. Trends Plant Sci. *15*, 395–401.

Santner, A., and Estelle, M. (2010). The ubiquitin-proteasome system regulates plant hormone signaling. Plant J. *61*, 1029–1040.

Sato, A., Sato, Y., Fukao, Y., Fujiwara, M., Umezawa, T., Shinozaki, K., Hibi, T., Taniguchi, M., Miyake, H., Goto, D.B., and Uozumi, N. (2009). Threonine at position 306 of the KAT1 potassium channel is essential for channel activity and is a target site for ABA-activated SnRK2/OST1/SnRK2.6 protein kinase. Biochem. J. *424*, 439–448.

Singer, J.D., Gurian-West, M., Clurman, B., and Roberts, J.M. (1999). Cullin-3 targets cyclin E for ubiquitination and controls S phase in mammalian cells. Genes Dev. *13*, 2375–2387.

Sirichandra, C., Gu, D., Hu, H.C., Davanture, M., Lee, S., Djaoui, M., Valot, B., Zivy, M., Leung, J., Merlot, S., and Kwak, J.M. (2009). Phosphorylation of the Arabidopsis AtrbohF NADPH oxidase by OST1 protein kinase. FEBS Lett. *583*, 2982–2986.

Sirichandra, C., Davanture, M., Turk, B.E., Zivy, M., Valot, B., Leung, J., and Merlot, S. (2010). The Arabidopsis ABA-activated kinase OST1 phosphorylates the bZIP transcription factor ABF3 and creates a 14-3-3 binding site involved in its turnover. PLoS ONE *5*, e13935.

Smalle, J., and Vierstra, R.D. (2004). The ubiquitin 26S proteasome proteolytic pathway. Annu. Rev. Plant Biol. *55*, 555–590.

Smalle, J., Kurepa, J., Yang, P., Emborg, T.J., Babiychuk, E., Kushnir, S., and Vierstra, R.D. (2003). The pleiotropic role of the 26S proteasome subunit RPN10 in Arabidopsis growth and development supports a substrate-specific function in abscisic acid signaling. Plant Cell *15*, 965–980.

Söderman, E., Hjellström, M., Fahleson, J., and Engström, P. (1999). The HD-Zip gene ATHB6 in Arabidopsis is expressed in developing leaves, roots and carpels and up-regulated by water deficit conditions. Plant Mol. Biol. *40*, 1073–1083.

Song, C.P., Agarwal, M., Ohta, M., Guo, Y., Halfter, U., Wang, P., and Zhu, J.K. (2005). Role of an Arabidopsis AP2/EREBP-type transcriptional repressor in abscisic acid and drought stress responses. Plant Cell *17*, 2384–2396.

Stogios, P.J., Downs, G.S., Jauhal, J.J., Nandra, S.K., and Privé, G.G. (2005). Sequence and structural analysis of BTB domain proteins. Genome Biol. *6*, R82.

Stone, S.L., Williams, L.A., Farmer, L.M., Vierstra, R.D., and Callis, J. (2006). KEEP ON GOING, a RING E3 ligase essential for Arabidopsis growth and development, is involved in abscisic acid signaling. Plant Cell *18*, 3415–3428.

Thomann, A., Brukhin, V., Dieterle, M., Gheyeselinck, J., Vantard, M., Grossniklaus, U., and Genschik, P. (2005). Arabidopsis CUL3A and CUL3B genes are essential for normal embryogenesis. Plant J. *43*, 437–448.

Thomas, J.H. (2006). Adaptive evolution in two large families of ubiquitin-ligase adapters in nematodes and plants. Genome Res. *16*, 1017–1030.

Thompson, J.D., Gibson, T.J., Plewniak, F., Jeanmougin, F., and Higgins, D.G. (1997). The CLUSTAL_X windows interface: flexible strategies for multiple sequence alignment aided by quality analysis tools. Nucleic Acids Res. *25*, 4876–4882.

Ton, J., Flors, V., and Mauch-Mani, B. (2009). The multifaceted role of ABA in disease resistance. Trends Plant Sci. *14*, 310–317.

Vierstra, R.D. (2009). The ubiquitin-26S proteasome system at the nexus of plant biology. Nat. Rev. Mol. Cell Biol. *10*, 385–397.

Weber, H., and Hellmann, H. (2009). Arabidopsis thaliana BTB/ POZ-MATH proteins interact with members of the ERF/AP2 transcription factor family. FEBS J. *276*, 6624–6635.

Weber, H., Bernhardt, A., Dieterle, M., Hano, P., Mutlu, A., Estelle, M., Genschik, P., and Hellmann, H. (2005). Arabidopsis AtCUL3a and AtCUL3b form complexes with members of the BTB/POZ-MATH protein family. Plant Physiol. *137*, 83–93.

Xu, L., Wei, Y., Reboul, J., Vaglio, P., Shin, T.H., Vidal, M., Elledge, S.J., and Harper, J.W. (2003). BTB proteins are substrate-specific adaptors in an SCF-like modular ubiquitin ligase containing CUL-3. Nature *425*, 316–321.

Yamaguchi-Shinozaki, K., and Shinozaki, K. (1993). Characterization of the expression of a desiccation-responsive rd29 gene of Arabidopsis thaliana and analysis of its promoter in transgenic plants. Mol. Gen. Genet. *236*, 331–340.

Yamaguchi-Shinozaki, K., and Shinozaki, K. (2006). Transcriptional regulatory networks in cellular responses and tolerance to dehydration and cold stresses. Annu. Rev. Plant Biol. *57*, 781–803.

Zhang, Q., Zhang, L., Wang, B., Ou, C.Y., Chien, C.T., and Jiang, J. (2006). A hedgehog-induced BTB protein modulates hedgehog signaling by degrading Ci/Gli transcription factor. Dev. Cell *10*, 719–729.

Zhuang, M., Calabrese, M.F., Liu, J., Waddell, M.B., Nourse, A., Hammel, M., Miller, D.J., Walden, H., Duda, D.M., Seyedin, S.N., et al. (2009). Structures of SPOP-substrate complexes: insights into molecular architectures of BTB-Cul3 ubiquitin ligases. Mol. Cell *36*, 39–50.